Springer

KSME

Journal of Mechanical Science and Technology 29 (4) (2015) 1715~1722
www.springerlink.com/content/1738-494x
DOI 10.1007/s12206-015-0344-2

Numerical analysis of weld pool oscillation in laser welding †

Jungho Cho[1,*], Dave F Farson[2], Kendall J Hollis[3] and John O. Milewski[3]

[1]*School of Mechanical Engineering, Chungbuk National University, Cheongju, 362-763, Korea*
[2]*IWSE, The Ohio State University, 1248 Arthur E Adams Drive, Columbus, OH 34221, USA*
[3]*Los Alamos National Laboratory, PO Box 1663, MS G770, Los Alamos, NM 87545, USA*

(Manuscript Received October 27, 2014; Revised December 4, 2014; Accepted December 16, 2014)

Abstract

Volume of fluid (VOF) numerical simulation was used to investigate melt flow and volumetric oscillation of conduction-mode pulsed laser weld pools. The result is compared to high speed video stream of titanium laser spot welding experiment. The total simulation time is 10ms with the first 5 ms being heating and melting under constant laser irradiation and the remaining 5 ms corresponding to re-solidification of the weld pool. During the melting process, the liquid pool did not exhibit periodic oscillation but was continually depressed by the evaporation recoil pressure. After the laser pulse, the weld pool was excited into volumetric oscillation by the release of pressure on its surface and oscillation of the weld pool surface was analyzed. The simulation model suggested adjusting thermal diffusivity to match cooling rate and puddle diameter during solidification which is distinguishable from previous weld pool simulation. The frequency continuously increased from several thousand cycles per second to tens of thousands of cycles per second as the weld pool solidified and its diameter decreased. The result is the first trial of investigation of small weld pool oscillation in laser welding although there have been several reports about arc welding.

Keywords: Laser; Welding; Weld pool; Oscillation; Simulation; VOF (Volume of fluid)

1. Introduction

It is easy to see ripples pattern on the top bead of the weldment after arc or laser welding process. The mechanism of the ripple formation is revealed as mainly due to the oscillation of weld pool during the solidification process [1] in gas tungsten arc (GTA) welding process. In the referred paper, the oscillation of the weld pool surface observed through high speed video is compared to the counted number of ripples. Another GTA weld pool observation research [2] tried to explain the geometric information of the solidified weld nugget by measured oscillation frequency.

Noticeable result in this field is reported in 1990 [3] which also investigated the GTA weld pool. In this article, arc voltage is measured and the achieved oscillation showed well matched result to the previous theoretical equation of the puddle. Following research [4] indicated the possibility of distinction between partial and full penetration in-process monitoring by measuring oscillation frequency because the frequency of full penetration is much smaller than that of partial case. Therefore, if one catches the sudden transition of puddle oscillation frequency from hundreds Hz of order to tens, full penetration can be detected in-process. Finally, weld pool oscillation is used to sense the penetration of work piece during the pulsed GTA welding process [5] with successful result. The same group also investigated the relationship between weld pool oscillation and stability of short circuit gas metal arc welding (GMAW) resulted as the most stable condition is when short circuit frequency is same to pool's oscillation frequency [6]. Another try for the penetration control was in 1994 using optical sensor to detect the oscillation [7] and it proposed penetration control system itself.

Research about the pool oscillation for the laser welding process has not been done much comparing to arc welding process. Because the laser welding pool is much smaller than the arc welding pool so it shows much higher frequency. Therefore, it is hard detect the oscillation due to the small size and cost of higher time resolution of high speed camera. Postacioglu et al. [8, 9] reported two theoretical research papers about the pool oscillation in laser welding. They made a cylindrically symmetric two dimensional mathematical model then derived natural frequencies of the pool for asymmetric and radially symmetric modes in their first report. And they developed their model to asymmetric ellipsoidal geometry for the high speed welding case. Semak et al. [10] used high speed video camera to detect the oscillation of the laser weld pool but it was mainly about the keyhole opening and closing

*Corresponding author. Tel.: +82 43 261 2445, Fax.: +82 43 263 2441
E-mail address: junghocho@cbnu.ac.kr
† Recommended by Associate Editor Young Whan Park

phase. Another interesting research was reported for about forced oscillation of keyhole [11] which means that the laser power is fluctuated then it made the keyhole oscillate in radial direction.

Mechanism of bead formation including flow pattern inside of the weld pool always has been curious in welding research area because it helps to derive ideas of preventing many kinds of defects such as pores, undercut and spatters.

In this research, fully three-dimensional titanium weld pool simulation is achieved to observe the oscillation of the free surface by using commercial solver Flow3D. Low power pulsed laser is applied as surface heat flux and famous volume of fluid (VOF) [12] method is adopted to track the free surface of the molten pool [13-15]. Applied laser pulse width is 5 ms but there is totally 10 ms of simulation time to give the model to be re-solidified. Then it is compared to titanium laser spot welding experiment which is recorded through high speed video system.

2. Governing equations and boundary conditions

The laser welding simulation was based on fluid dynamics conservation laws, discretized on a regular three-dimensional spatial array in Cartesian coordinates and solved by the finite difference method. The three-dimensional continuity equation expressing conservation of volume for the flow of an incompressible fluid is

$$\nabla \cdot \vec{V} = 0. \tag{1}$$

The molten metal viscosity was assumed to be Newtonian and fluid flow was assumed as laminar. For these conditions, conservation of momentum including viscous stress is expressed as [16].

$$\frac{D\vec{V}}{Dt} = -\frac{1}{\rho}\nabla P + \mu\nabla^2\vec{V} + \vec{G}_z\left[1-\beta\left(T-T_m\right)\right]. \tag{2}$$

The final term in Eq. (2) represents the buoyant acceleration due to thermal expansion of the fluid, the volume changes of which are assumed to be small enough to be negligible in Eq. (1) (Boussinesq approximation). The VOF technique is based on the variable F, a scalar denoting the volume fraction of fluid occupying each simulation element (Cubic, in this simulation). By definition, with the extreme values occurring in void and fluid elements respectively and the intermediate values occurring in free surface elements. Conservation of F is expressed as

$$\frac{DF}{Dt} = \frac{\partial F}{\partial t} + \nabla\cdot\left(\vec{V}F\right) = 0. \tag{3}$$

In free surface fluid dynamics simulations, welding heat input is imposed as a surface heat flux boundary condition and the energy is convected and conducted throughout the weld pool and solid material. The present simulation considered only conservation of thermal energy in the weld pool- the kinetic and potential energies of the flow of molten material were assumed negligible in comparison. The relevant expression that includes melting enthalpy is

$$\frac{dh}{dt} + \left(\vec{V}\cdot\nabla\right)h = \frac{1}{\rho}\nabla\cdot\left(K\nabla T\right) \tag{4}$$

$$h = C_p\cdot T + f(T)\cdot L_f \tag{5}$$

$$f\left(T\right) = \begin{cases} 0, & if\ T < T_m \\ 1, & if\ T \geq T_m \end{cases}. \tag{6}$$

The laser beam irradiance was modeled as a Gaussian function

$$q(x,y) = \frac{3Q}{\pi r_L^2}exp\left(-3\frac{x^2+y^2}{r_L^2}\right). \tag{7}$$

The coefficient value of 3 implies that 95% of the total energy exists inside of the effective laser beam radius.

Weld pool surface heat fluxes due to heating by laser irradiation and cooling by air convection, thermal radiation and evaporation were applied to the upper free surface of the work piece according to the expression

$$K\frac{\partial T}{\partial n} = \eta q - h_A\left(T-T_\infty\right) - \sigma_s\varepsilon_r\left(T^4 - T_\infty^4\right) - q_{vap}. \tag{8}$$

The laser absorptivity η in Eq. (11) was estimated as a function of surface temperature according to the Ref. [17] and it is expressed like the following.

$$\eta = 354.67\sqrt{\rho} \tag{9}$$

$$\rho = 10^{-8}\left(a+bT\right). \tag{10}$$

Eq. (9) is valid for laser energy wavelength of 1.03μm. The constants in Eq. (10) for the temperature-varying resistivity of metal were a = 22.1 and b = 0.11 in the temperature range 273-1150K (varied from 0.25 to 0.432 in this range) and a = 148.6 and b = 0 in the range 1150-1953K. Therefore the absorptivity starts from 0.25 and ramps up to 0.432 until liquid phase then maintained in that value. The authors used 0.12 higher absorptivity to match the penetration depth and bead width and more detailed description will be appeared in discussion chapter.

Surface evaporation is the defining characteristic of high power laser beam welding. Evaporation has prominent thermal and mechanical effects that become stronger as surface temperature is increased. Evaporation from liquid metal surfaces under intense laser irradiance has been much analyzed and this work used relationships established by the extensive

prior investigations [18-22]. In analysis of evaporation at high irradiance, it is commonly assumed that vapor evolves at sonic velocity from a Knudsen layer adjacent to the molten surface. Applying conservation and kinetics laws across this vapor flow discontinuity allows relevant thermal and pressure boundary conditions to be calculated for the weld pool surface.

The evaporation cooling is expressed as

$$q_{vap} = 0.82\frac{\Delta H^*}{\sqrt{2\pi MRT}}P_0 exp\left(\Delta H^*\frac{T-T_{LV}}{RTT_{LV}}\right) \quad (11)$$

where enthalpy of vapor flowing at sonic velocity is

$$\Delta H^* = \Delta H_{LV} + \frac{\gamma(\gamma+1)}{2(\gamma-1)}RT\,. \quad (12)$$

In laser welding, one of the main driving forces for melt pool flow is the pressure exerted by the metal vapor expanding freely from the molten pool surface (Recoil pressure). An expression for recoil pressure as a function of liquid surface temperature is

$$P_r = 0.54P_0 exp\left(\Delta H_{LV}\frac{T-T_{LV}}{RTT_{LV}}\right). \quad (13)$$

The boundary condition for pressure normal to the free surface is

$$-P + 2\mu\frac{\partial V_n}{\partial n} = -P_r + \gamma_s\left(\frac{1}{R_x}+\frac{1}{R_y}\right). \quad (14)$$

The pressure BC expressed by Eq. (14) includes the recoil pressure and surface tension force.

To model Marangoni flow, the shear stress balance as boundary condition on the free surface is described as

$$\mu\frac{\partial V_\tau}{\partial n} = -\frac{\partial\gamma_s}{\partial T}\frac{\partial T}{\partial\tau}\,. \quad (15)$$

Boundary conditions for the area of the surface outside of the laser heat input were set as continuative (All flow properties have zero normal derivative). Analytic domain is set as three-dimensional rectangle and some top portion of the rectangle is set as empty which means the volume fraction in this region is zero in VOF technique. This empty space is for the bumped up and depressed free surface of the weld pool. Width and length of the rectangle are both set as 1.6 mm. The height is 0.7 mm and 0.2 mm of it is set as empty to observe the free surface of the molten pool. Grid size is set as 0.02 mm for all three axes. Therefore, there are 224000 cells in the domain. Material of the simulation is commercially pure titanium and its thermo-physical properties are shown in Table 1. Values of the coefficients and constants used in the simulation are also appeared in the same table.

Table 1. Thermo-physical properties of titanium and coefficients and constants used in the simulation.

Name	Symbol	Value
Density	ρ	4110 kg/m^3
Viscosity	μ	5.2×10^{-5} kg/m·s
Thermal conductivity	K	40 W/m·K
Surface tension	γ_s	1.65 N/m
Thermal sensitivity of surface tension	-	2.6×10^{-5}
Specific heat	C_p	594 J/kg·K
Melting point	T_m	1953 K
Boiling point	T_{LV}	3562 K
Latent heat of fusion	L_f	403 kJ/kg
Latent heat of vaporization	ΔH_{LV}	8828.8 kJ/kg
Emissivity	ε_r	0.8
Stefan-Boltzmann constant	σ_s	5.67×10^{-8} W/m^2·K^4
Convection coefficient	h_A	80 W/m^2
Molar mass	M	0.0479 kg/mol
Universal gas constant	R	8.3144 J/K·mol
Temperature of environment	T_∞	293 K

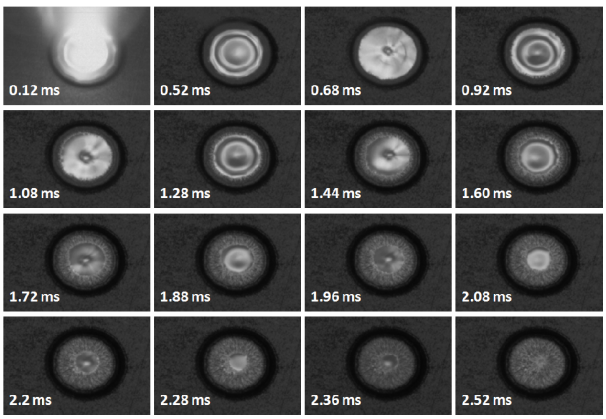

Fig. 1. Sequential images of weld pool oscillation after laser pulse off.

3. Results and discussions

Laser spot welding on 0.5 mm thickness titanium is conducted and compared to simulation. The laser pulse had 3.3 J energy and 5 ms pulse width therefore square shaped pulse which has 660 W peak power is assumed and applied to simulation. The weld pool of experiment is recorded through high speed video system. It has 0.04 ms time interval between single images. Therefore, the maximum resolution of measurable frequency of experimental weld pool oscillation is 12.5 kHz according to Shannon's sampling theorem. Captured single images are shown in Fig. 1. The video is not captured syn-

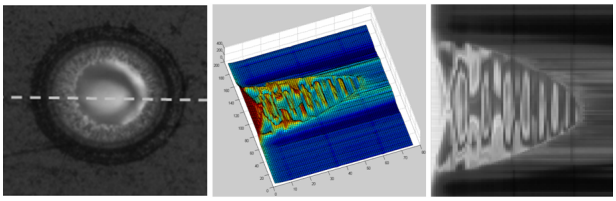

(a) Center line intensity (b) Stacked data in 3D (c) Stacked data in 2D

Fig. 2. Center line pixels intensity profile stacked in time sequence.

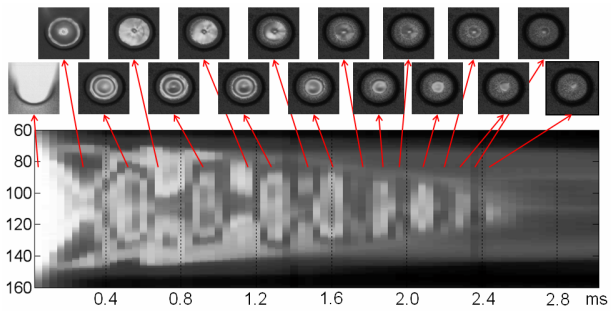

Fig. 3. 3D weld pool oscillation data and its corresponding image.

chronously with laser pulse triggering therefore 0.12 ms in Fig. 1 is from the selected images and believed right just after laser pulse off because the vapor plume behavior is noticeably reduced. During laser pulse on period, video images show all brightness caused by metal vapor plume. Even counting on one or two images before 0.12 ms moment in here, total re-solidification time is below 2.5 ms. As seen in the figure, weld pool fluctuation is clearly captured through the high speed video. The moments of peak and valley of oscillation are selected before full re-solidification and shown in Fig. 1. There are totally 8 or 9 fluctuations observed through pictures. One thing noticeable is that the time period between consecutive peaks or valleys is getting shorter along solidification process which means increase of oscillation frequency. Through the selected pictures, the last two dimple shape shows 0.2 ms time difference (2.28 ms-2.08 ms), therefore the oscillation frequency right just before solidification is approximately 5 kHz.

Fig. 2 is a unique presentation of the weld pool oscillation in video stream. The centerline's pixel intensity of weld pool image is stacked in a row along time. The three dimensional display of this data is seen in Fig. 2(b) and two dimensional image is seen in Fig. 2(c). This kind of map is quite efficient to show weld pool oscillation with respect to time through only one figure. Each column in Fig. 2(c) means one time interval between single images, 0.04 ms. Therefore the repetitive pattern in the picture represents the weld pool fluctuations.

In Fig. 3, stretched 2D weld pool oscillation data mentioned in above paragraph is shown and corresponding images are listed for selected columns. The images in this figure can be categorized in two types, one is the dimple shape which will be referred as valley moment from now for the convenience and the other type will be peak moment. The first peak is observed in 0.28 ms moment and the next one is in 0.68 ms, therefore

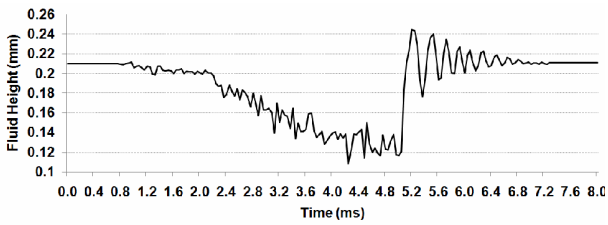

Fig. 4. Fluctuation of fluid center height in simulation result.

the initial oscillation frequency is assumed as 2.5 kHz. The amplitude of weld pool oscillation of the experiment is not independently measured so the exact moment of peak and valley is not given except for this rough approximation based on images. However, one can presume the each period of fluctuation through the map displayed in Fig. 3. There are 8 observable pictures of peak and valley for each and the highest frequency is appeared at the last, right just before full solidification. It has only two time step difference, 0.08 ms, computed as 12.5 kHz which corresponds to the limit of achievable frequency by the video measurement mentioned in above. Qualitatively speaking, decreasing weld pool diameter during solidification and increasing oscillation frequency in reverse of diameter are observed through the map and pictures in Fig. 3.

Simulation model successfully showed the weld pool fluctuation. To present the oscillation, weld pool center's height is recorded according to time and shown in Fig. 4 for whole simulation time. The flat region in the graph indicates no fluctuation therefore it is deduced that the melting starts from around 0.8 ms and re-solidification is completed around after 7.4 ms. The pool height is continuously decreasing while laser pulse is on and the maximum deformation is observed as about 0.1 mm. During the melting process, that is to say, until 5 ms, weld pool shows irregular fluctuation caused by complex interaction between recoil pressure, surface tension and massive pool dynamics. However, after role of recoil pressure is removed, pool surface starts to show clear oscillation like the graph after 5 ms. The amplitude is continuously decreasing along pool diameter decrease then soon disappeared with the completion of re-solidification.

The cross sectional images of fluctuation of weld pool are seen in Fig. 5. It is known that HAZ (heat affected zone) of titanium exists between α/β transition isotherm (1158 K) and the liquidus temperature (1953 K) therefore the temperature scale is set according to it. The series of pictures show the first four fluctuations after laser pulse off. At the moment of 5 ms, deformed weld pool and downward central flow due to recoil pressure is clearly observed. Titanium in this simulation and experiment is commercially pure one therefore the fluid has negative temperature sensitivity of surface tension. However, typical outward Maragoni surface flow is hard to figure out, except for the top solid/liquid boundary region in the pictures because of overwhelming recoil pressure effect. When the laser surface heat flux is removed, the recoil pressure quickly lost its power then the volumetric oscillation of weld pool is

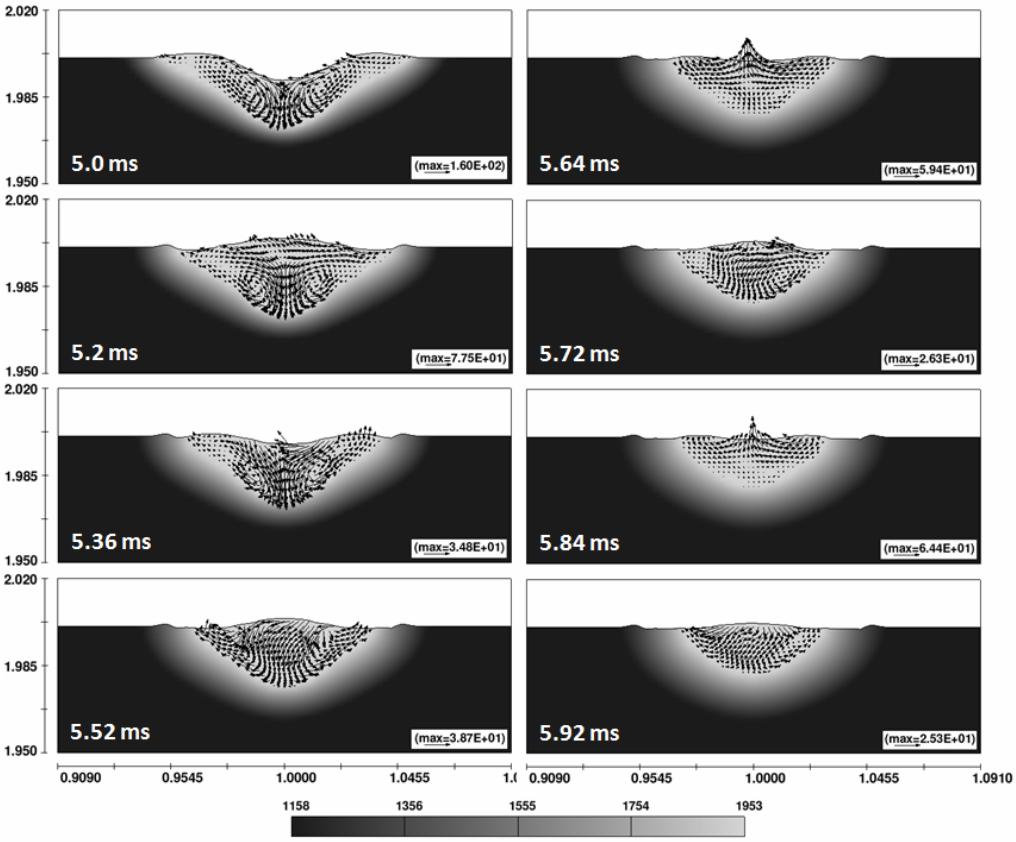

Fig. 5. Sequential images of weld pool oscillation right just after laser pulse off.

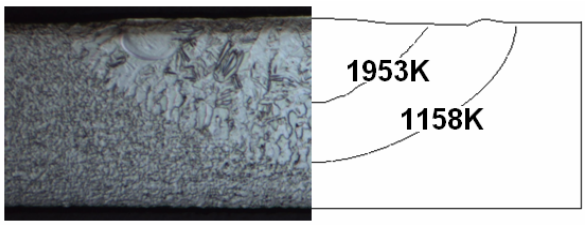

Fig. 6. Comparison of experiment and simulation result.

begun like the series of pictures. It is noticeable that the time interval between fluctuation valleys is getting shorter along solidification process. The first interval, between first and third picture in left column, is 0.36 ms and then it is changed to 0.28 ms and 0.2 ms. It is showing increasing frequency of weld pool oscillation with respect to decreasing pool diameter.

Cross section of experiment and simulation is directly compared in Fig. 6. In commercially pure titanium welding picture, it is difficult to distinguish FZ (Fusion zone) directly if microscopic structure is not inspected as seen in the figure. However, HAZ is clearly distinctive from base metal. Therefore the HAZ in cross section and pool diameter in high speed video are focused to tune simulation model. Fig. 6 shows comparatively well matched simulation result to experiment. It is common to tune the parameters such as laser absorptivity or conductivity to match the simulation to experiment [23, 24]. The conductivity of the metal is actually varied along temperature and liquid conductivity is much higher than solid state. Therefore, using higher conductivity than that of room temperature is not strange thing at all. It is also well known fact that the metal's laser absorptivity varies with respect to surface condition and temperature [25-29]. In this research, the simulation model used the previous result of temperature dependent laser absorptivity and 0.12 more than that to match the weld and HAZ size. The conductivity is doubled comparing to room temperature's to match the cooling rate by adjusting thermal diffusivity. Unlike other weld pool simulations, matching cooling rate is very important in this research because the oscillation is highly dependent on the pool size. Well matched cooling rate is shown in Fig. 7. Weld pool's top diameter of simulation and experiment is measured along time compared each other.

The fluctuation of weld pool after laser pulse off is especially displayed in Fig. 8. In this figure, fluid center height is recorded for every 0.01 ms therefore the measurable maximum frequency is 50 kHz. And the highest frequency of oscillation is observed as around 20 kHz near 6.9 ms. The free surface of every up and down moment during solidifying oscillation is shown. Repetitive convex and concave shapes are observable until time reach 6.4ms, after this, it is hard to figure

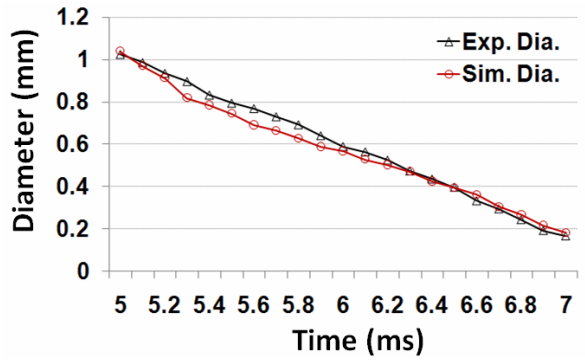

Fig. 7. Weld pool diameter change in experiment vs. simulation.

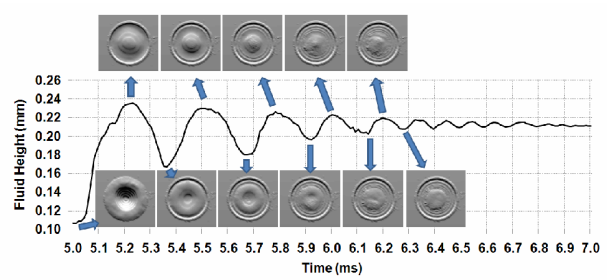

Fig. 8. Fluctuation of weld pool center during solidification and top surface view for each peak and valley.

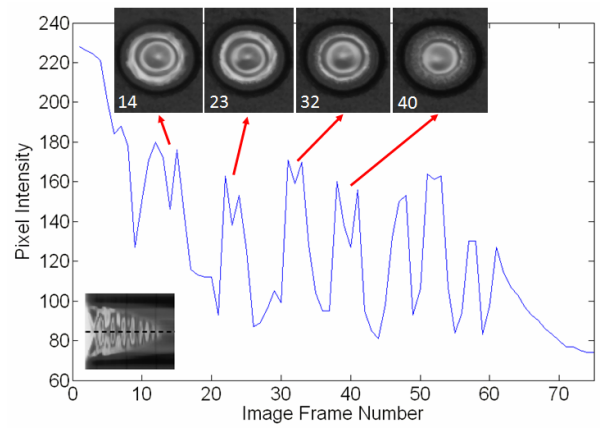

Fig. 9. Time sequential center point intensity profile and corresponding images.

out the fluctuation from the shape. Thanks to the precise free surface tracking, circular ripples of the weld are observed after solidification. As the previous report said [1, 2], one ripple is made after one fluctuation and radial distance between ripples are getting shorter along the frequency increase. However, the ripples are not observable anymore after the pool diameter is smaller than around 0.5 mm. In the fluctuation graph of the figure, small fluctuation of high frequency is observed which could be free surface tracking error or high frequency oscillation or sloshing. But, it was hard to detect what it is graphically like the picturs because the amplitude is too small. One clue is that the experiment shows similar minor fluctuation phenomenon like Fig. 9. The graph in this figure is the intensity profile of center point because it is horizontal centerline's profile of the map in Figs. 2 and 3. In Fig. 9, small fluctuation is also observed in every peak region. If it were perfectly smooth fluctuation, the graph would also show smooth fluctuation not like Fig. 9. Therefore, it is believed that high frequency oscillation exists inside of the relatively low frequency oscillation which is not clearly observed through images.

There have been reports [3-6] about the weld pool oscillation frequency. It used membrane's frequency formula then showed well matched result with the arc weld pool. The team of this research also tried to apply the membrane's frequency formula to experiment and simulation. However, it showed much higher frequency than observation of experiment and simulation. The membrane approximation well matched to arc weld pool which has diameter range between 3 mm and 10 mm. But it is revealed that the membrane's formula is not appropriate for the laser weld pool in this research has diameter below 1 mm.

4. Conclusions

Proposed full 3D numerical analysis model in this research successfully reproduced the weld pool oscillation through computer simulation. Thermo physical parameters such as laser absorptivity and thermal conductivity of titanium are tuned to match the weld size and cooling rate to experimental result. The oscillation frequency during solidification process, after pulsed laser off, is not conservative but varies along the weld pool diameter decrease. The trend is similar to the previous report about arc weld pool oscillation which adopted theoretical membrane's vibration model to explain the puddle frequency. However the result in this research revealed that the previous arc pool oscillation model is not appropriate for the laser weld pool whose diameter, 1mm, is very small comparing to arc pool.

Acknowledgement

This research was supported by Basic Science Research Program through the National Research Foundation of Korea (NRF) funded by the Ministry of Science, ICT and Future Planning (Grant No. 2012R1A1A1012487).

Nomenclature

C_p : Specific heat
F : Volume fraction in the VOF cell
G_z : Gravitational acceleration in z direction
h : Enthalpy
h_A : Convection coefficient
K : Thermal conductivity
L_f : Latent heat of fusion
M : Molar mass
P : Pressure

P_0 : Atmospheric pressure
P_r : Recoil pressure
Q : Nominal laser power
R : Universal gas constant
R_x, R_y : Principal radii of local curvature of free surface
r_L : Effective radius of laser
T : Temperature
t : Time
T_m : Melting temperature
T_{LV} : Boiling temperature
T_∞ : Temperature of environment
V : Velocity
$\vec{V}$: Velocity vector
ΔH_{LV} : Latent heat of vaporization

Greek symbols

β : Volume thermal expansion coefficient
γ : Adiabatic index
γ_s : Aurface tension
ε_r : Emissivity
η : Laser absorptivity
μ : Viscosity
ρ : Density, resistivity
σ_s : Stefan-Boltzmann constant

Superscripts, subscripts

n : Normal component
τ : Surface tangent direction
x, y, z : Cartesian coordinate index

References

[1] D. J. Kotecki, D. L. Cheever and D. G. Howden, Mechanism of ripple formation during weld solidification, *Welding Journal*, 51 (1972) 386s-391s.

[2] R. J. Renwick and R. W. Richardson, Experimental investigation of GTA weld pool oscillations, *Welding Journal*, 62 (1983) 29s-35s.

[3] Y. H. Xiao and G. D. Ouden, A study of GTA weld pool oscillation, *Welding Journal*, 69 (1990) 289s-293s.

[4] Y. H. Xiao and G. D. Ouden, Weld pool oscillation during GTA welding of mild steel, *Welding Journal*, 72 (1993) 428s-434s.

[5] A. J. R. Aendenroomer and G. D. Ouden, Weld pool oscillation as a tool for penetration sensing during pulsed GTA welding, *Welding Journal* (1998) 181s-187s.

[6] M. J. M. Hermans and G. D. Ouden, Process behavior and stability in short circuit gas metal arc welding, *Welding Journal*, 78 (1999) 137s-141s.

[7] K. Andersen, G. E. Cook, R. J. Barnett and A. M. Strauss, Synchronous weld pool oscillation for monitoring and control, *IEEE Transactions on Industrial Applications*, 33 (1997) 464-471.

[8] N. Postacioglu, P. Kapadia and J. Dowden, Capillary waves on the weld pool in penetration welding with a laser, *Journal of Physics D: Applied Physics*, 22 (1989) 1050-1061.

[9] N. Postacioglu, P. Kapadia and J. Dowden, Theory of the oscillation of an ellipsoidal weld pool in laser welding, *Journal of Physics D: Applied Physics*, 24 (1991) 1288-1292.

[10] V. V. Semak, J. A. Hopkins, M. H. McCay and T. D. McCay, Melt pool dynamics during laser welding, *Journal of Physics D: Applied Physics*, 28 (1995) 2443-2450.

[11] T. Klein, M. Vicanek and G. Simon, Forced oscillations of the keyhole in penetration laser beam welding, *Journal of Physics D: Applied Physics*, 29 (1996) 322-332.

[12] C. W. Hirt and B. D. Nichols, Volume of Fluid (VOF) Method for the Dynamics of Free Boundaries, *Journal of Computational Physics*, 39 (1981) 201-225.

[13] J. H. Cho and S. J. Na, Implementation of real-time multiple reflection and Fresnel absorption of laser beam in keyhole, *Journal of Physics D: Applied Physics*, 39 (2006) 5372-5378.

[14] J. H. Cho and S. J. Na, Theoretical analysis of keyhole dynamics in polarized laser drilling, *Journal of Physics D: Applied Physics*, 40 (2007) 7638-7647.

[15] J. H. Cho, D. F. Farson, J. O. Milewski and K. J. Hollis, Weld pool flows during initial stages of keyhole formation in laser welding, *Journal of Physics D: Applied Physics*, 42 (2009) 175502.

[16] R. W. Fox and A. T. McDonald, *Introduction to fluid mechanics*, 4th ed., John Wiley & Sons, Inc. (1992).

[17] J. Xie, A. Kar, J. A. Rothenflue and W. P. Latham, Temperature-dependent absorptivity and cutting capability of CO2, Nd:YAG and chemical oxygen-iodine lasers, *Journal of Laser Applications*, 9 (1997) 77-85.

[18] C. J. Knight, Theoretical modeling of rapid surface vaporization with back pressure, *The American Institute of Aeronautics and Astronautics Journal*, 17 (1979) 519-523.

[19] S. I. Anisimov, Vaporization of metal absorbing laser radiation, *Journal of Experimental and Theoretical Physics*, 27 (1968) 182-183.

[20] M. von Allmen and A. Blatter, *Laser-beam interactions with materials: physical principles and applications*, 2nd ed., Berlin, Springer (1987).

[21] T. E. Itina, J. Hermann, P. Delaporte and M. Sentis, Laser-generated plasma plume expansion: Combined continuous-microscopic modeling, *Physics Review E*, 66 (2002) 066406.

[22] V. Semak and A. Matsunawa, The role of recoil pressure in energy balance during laser materials processing, *Journal of Physics D: Applied Physics*, 30 (1997) 2541-2552.

[23] A. De and T. DebRoy, A smart model to estimate effective thermal conductivity and viscosity in the weld pool, *Journal of Applied Physics*, 95 (2004) 5230-5240.

[24] J. F. Lancaster, The physics of welding, *Physics in Technology*, 15 (1984) 73-79.

[25] J. T. Wang, C. I. Weng, J. G. Chang and C. C. Hwang, The influence of temperature and surface conditions on surface absorptivity in laser surface treatment, *Journal of Applied*

Physics, 87 (2000) 3245-3253.
[26] D. Bergström, J. Powell and A. F. H. Kaplan, A ray-tracing analysis of the absorption of light by smooth and rough metal surfaces, *Journal of Applied Physics*, 101 (2007) 113504.
[27] J. M. Elson and C. C. Sung, Intrinsic and roughness-induced absorption of electromagnetic radiation incident on optical surfaces, *Applied Optics*, 21 (1982) 1496-1501.
[28] K. Ujihara, Reflectivity of metals at high temperature, *Journal of Applied Physics*, 43 (1972) 2376-2383.
[29] A. I. Korotchenko, A. A. Samokhin and A. B. Uspenskii, Behavior of the absorptivity of metals under the action of laser radiation, *Soviet Journal of Quantum Electronics*, 9 (1979) 115-119.

Jungho Cho received his Ph.D. at KAIST in 2007 and now he is a faculty of Chungbuk National University after working at Hyundai Motors for several years. His major is development of welding and joining techniques, welding physics and thermo-dynamical analysis of weld pool.